

# DESIGNING OPTIMAL PULSE-SHAPERS FOR ULTRA-WIDEBAND RADIOS

Xiliang Luo, Liuqing Yang, and Georgios B. Giannakis

Dept. of ECE, Univ. of Minnesota, 200 Union Street SE, Minneapolis, MN 55455

## ABSTRACT

Ultra-Wideband (UWB) technology is gaining increasing interest for its potential application to short-range indoor wireless communications. Utilizing ultra-short pulses, UWB baseband transmissions enable rich multipath diversity, and can be demodulated with low complexity receivers. Compliance with the FCC spectral mask, and interference avoidance to, and from, co-existing narrow-band services, calls for judicious design of UWB pulse shapers. This paper introduces pulse shaper designs for UWB radios, which optimally utilize the bandwidth and power allowed by the FCC spectral mask. The resulting baseband UWB systems can be either single-band, or, multi-band. More important, the novel pulse shapers can support dynamic avoidance of narrow-band interference, as well as efficient implementation of fast frequency hopping, without invoking analog carriers.

## 1. INTRODUCTION

UWB radio is gaining increasing interest for its potential in short-range indoor wireless communications. Utilizing ultra-short pulses, UWB baseband transmissions enable rich multipath diversity, and can be demodulated with low complexity receivers.

Occupying extremely broad bandwidth, UWB radios inevitably overlay existing narrow-band services. To regulate co-existence, the FCC has released a spectral mask that limits the equivalent isotropic radiated power (EIRP) spectrum density, which depends critically on the UWB pulse shaper used. Unless the latter adheres to the FCC mask in a power-efficient manner, simply lowering the transmit power to limit interference trades-off receive SNR. The pulse shaper should also be configurable to avoid interference to (and from) co-existing services that reside in neighbouring bands. Unfortunately, the widely adopted Gaussian monocycle is not flexible enough to meet these requirements [2]. To design pulse shapers with desirable spectral properties, two approaches can be pursued: carrier-modulation and/or baseband analog/digital filtering of the baseband pulse shaper. The former relies on local oscillators at the UWB transceivers, which being prone to mismatch give rise to carrier frequency offset and jitter effects (CFO/CFJ). Shaping the Gaussian pulse with a baseband analog filter can avoid CFO/CFJ, but digital filters are certainly more flexible.

To this end, this paper introduces optimal pulse shapers for UWB using the “workhorse” of digital filter design methods, namely the Parks-McClellan algorithm [9]. The resulting pulse shapers exploit the FCC spectral mask optimally, and offer flexibility for (dynamic) avoidance of narrow-band interference (NBI). Furthermore, they are ideally suited for digital implementation of sub-band (or frequency) hopping (FH) codes, which are used with *multi-band* UWB systems. The latter have gained popularity recently, because they can replace the traditional time-hopping (TH) codes for multiple access (MA) [1], or, complement them to enhance capacity and covertness.

Pulse shapers respecting the FCC mask were also proposed in [3]. Unlike [3], our designs not only offer optimality in *meeting* the FCC mask, but also *optimally exploit* the allowable bandwidth and power. Moreover, implementing [3] entails D/A operations at 64GHz rate; whereas our designs can be implemented without modifying the analog components of existing UWB transceivers [2].

## 2. TRANSMIT SPECTRUM AND PULSE SHAPER

The typical modulation in UWB radios is binary pulse position modulation (PPM), in conjunction with TH codes that are used to enable MA and smooth the transmit-spectra [1]. With  $p(t)$  denoting the pulse shaper with energy  $\mathcal{E}_p$ , the emitted waveform from a single UWB transmitter is

$$u(t) = \sum_k \sqrt{\frac{\mathcal{E}}{\mathcal{E}_p}} p(t - kT_f - c_k T_c - s(\lfloor k/N_f \rfloor) \Delta), \quad (1)$$

where  $\mathcal{E}$  is the transmitted energy per pulse,  $T_f$  is the frame duration consisting of  $N_c$  chips,  $c_k \in [0, N_c - 1]$  is the  $N_f$ -periodic TH sequence,  $T_c$  is the chip period,  $s(n)$  represents the information symbol, and  $\Delta$  is the PPM modulation index. With  $k$  indexing frames in (1), each information symbol is transmitted over  $N_f$  frames, which explains the floor operation  $\lfloor k/N_f \rfloor$ . The transmit spectrum, i.e., the power spectrum density (PSD) of  $u(t)$  can be calculated as

$$\Phi_{uu}(f) = \frac{\mathcal{E}}{\mathcal{E}_p} \frac{1}{T_f} |P(f)|^2 \rho(f), \quad (2)$$

where  $\rho(f)$  depends on the TH codes chosen [4]. Although  $\rho(f)$  contains spectral spikes, the severity of interference from UWB transmissions to co-existing systems depends on the average power, which entails integration of the PSD over the band (say  $[f_1, f_2]$ ) that the victim system(s) operates in. For this reason,  $\rho(f)$  can be approximated as:  $\int_{f_1}^{f_2} \rho(f) df \approx f_2 - f_1$ , where  $f_2 - f_1 > 1/T_f$ . In other words, it is possible

The work in this paper was supported by the ARL/CTA Grant No. DAAD19-01-2-0011 and the NSF Grant No. EIA-0324864.

to approximate the EIRP spectrum of a single UWB transmitter as [c.f. (1)]

$$\Phi_{EIRP}(f) \cong \frac{\mathcal{E}}{\mathcal{E}_p} \frac{|P(f)|^2}{T_f}. \quad (3)$$

FCC requires that the EIRP spectra emitted by indoor UWB radios must adhere to the spectral mask depicted in Fig. 1 (left). In order to satisfy the FCC limit,  $\Phi_{EIRP}(f)$  must stay below the prescribed spectral mask. Evidently, this can be achieved for any  $p(t)$  by confining  $\mathcal{E}$  to sufficiently low values. But recall that symbol detection performance depends on the receive SNR, which is proportional to  $\mathcal{E}$ . It is thus desirable to design pulse shapers that allow for efficient exploitation of the FCC mask.

Before introducing our pulse shaper designs, let us first consider the Gaussian pulse that is widely adopted by UWB radar and communication systems [5]. With the Gaussian pulse as input, the UWB antenna acts as a differentiator [6] to produce at its output the first derivative of the Gaussian pulse, which is known as the Gaussian monocycle [2]. Since the transmit spectrum depends on the pulse shape at the output of the antenna, we will henceforth consider the pulse shaper incorporating the aggregate effects of the on-chip pulse in cascade with the transmit antenna. The Gaussian monocycle can be expressed as  $g(t) = 2\sqrt{e}A\frac{t}{\tau_g}e^{-2(\frac{t}{\tau_g})^2}$ , where  $\tau_g$  is the duration between its minimum and maximum values and  $A$  represents its peak amplitude. The pulse duration is approximately  $T_g = 4\tau_g$ . If  $G(f)$  denotes the Fourier Transform (FT) of  $g(t)$ , then  $|G(f)|$  is maximum at  $f_g := 1/(\pi\tau_g)$ .

Letting  $p(t) = g(t)$  in (1), the transmit EIRP spectrum is depicted in Fig. 1(left) with two values of transmission power: a prohibitively high power (System 1), and a sufficiently low power (System 2). Trying to maximize transmission power, System 1 violates the FCC spectrum mask; whereas trying to respect the FCC mask at the forbidden band, System 2 does not exploit the FCC mask in a power efficient manner. Consequently, the Gaussian monocycle does not lead to optimal utilization of the spectrum assigned by FCC. Moreover, utilization of the entire bandwidth entails circuits and processors with enormous frequency response. The payback, however, may not be as handsome, due to the increasingly lossy nature of high frequency bands. Therefore, it is sometimes desirable to use only a fraction of the entire bandwidth, which also facilitates NBI suppression. More important, partitioning the entire bandwidth, and letting each user utilize only a fraction of it, enables MA via FH. Although readily implementable [8], the Gaussian monocycle does not provide us with such capability and flexibility, unless it is employed after some processing. These considerations give rise to the following question:

*Using the Gaussian monocycle  $g(t)$ , that constitutes the antenna's physical response, as the elementary building block, can we optimally design  $p(t)$  with desirable spectral characteristics?*

### 3. OPTIMAL PULSE DESIGN

As mentioned before, the transmit EIRP spectrum  $\Phi_{EIRP} \propto |P(f)|^2$ . In order to utilize the FCC spectral mask efficiently,  $|P(f)|$  needs to closely approximate the shape of the spectral mask, which translates to a desired magnitude profile  $P_d(f)$ . We will show later that  $P_d(f)$  can be chosen to satisfy any desirable specifications. The problem statement is:  
*Given the Gaussian monocycle  $g(t)$  with  $\tau_g$  (or, equivalently,  $f_g$ ), and the desired FT magnitude  $P_d(f)$ , design  $p(t)$  so that  $|P(f)|$  approximates  $P_d(f)$  in some meaningful sense of optimality.*

Normalizing the square root of the FCC spectral mask to an FT mask  $\mathcal{M}(f)$  such that  $\max_f \mathcal{M}(f) = 1$  (see Fig. 1(center)), our desirable  $P_d(f)$  should be clearly upper bounded by  $\mathcal{M}(f)$ . Our approach to design  $p(t)$  is based on this model:

$$p(t) = \sum_{n=0}^{M-1} w[n]g(t - nT_0), \quad (4)$$

where  $w[n]$  are the tap coefficients with spacing  $T_0$  to be designed. As we will discuss later, the choice of  $T_0$  affects  $w[n]$ , and thus the feasibility, optimality, and complexity of the overall design. It can be easily verified that the FT of  $p(t)$  is given by [c.f. 4]:  $P(f) = W(e^{j2\pi f T_0})G(f)$ , where  $W(e^{j2\pi f T_0}) := \sum_{n=0}^{M-1} w[n]e^{-j2\pi f T_0 n}$ , which is periodic with period  $(1/T_0)$ Hz. Furthermore, requiring  $\{w[n]\}_{n=0}^{M-1}$  to be real,  $|W(e^{j2\pi f T_0})|$  must be symmetric with respect to  $f = 0$ . Hence, we can independently control  $|P(f)|$  by adjusting the weights  $w[n]$  only over the band  $[0, 1/(2T_0)]$ . This implies that, depending on the prescribed band of interest,  $T_0$  needs to be selected accordingly.

After careful selection of  $T_0$ , our  $p(t)$  design problem is:  
*Find  $M$  tap coefficients:  $\{w[n]\}_{n=0}^{M-1}$ , so that the function  $|W(e^{j2\pi f T_0})|$  satisfies:*

$$\begin{cases} |W(e^{j2\pi f T_0})| \approx \frac{P_d(f)}{|G(f)|}, & f \in [0, \frac{1}{2T_0}] \\ |W(e^{j2\pi f T_0})| < \frac{\mathcal{M}(f)}{|G(f)|}, & f \in [\frac{1}{2T_0}, +\infty] \end{cases} \quad (5)$$

Furthermore, if  $f_g$  is also specified, the pulse shaper design problem boils down to an FIR filter design problem:

*Design an  $M$ -tap FIR filter with coefficients:  $\{w[n]\}_{n=0}^{M-1}$ , so that its Discrete Time Fourier Transform (DTFT) magnitude  $|W(e^{j2\pi F})|$  approximates the function  $D(F/T_0)$ ,  $F \in [0, 0.5]$ , where  $D(f) := P_d(f)/|G(f)|$ ,  $f \in [0, \frac{1}{2T_0}]$ .*

Aiming at low complexity implementation, we wish to minimize the number of taps  $M$ , which in turn minimizes the duration of the resultant pulse shaper for a given  $T_0$ , since  $T_p = T_g + (M - 1)T_0$ . These considerations motivate us to adopt the Parks-McClellan algorithm [9], which leads to pulse shaper designs that are optimal in the sense that they minimize the maximum approximation error over the frequency band of interest. For simplicity, we choose linear phase filter approximants of order  $2L$  with symmetric taps, i.e.,  $w[n] = w[2L - n]$ ,  $\forall n$ . Instead of  $M =$

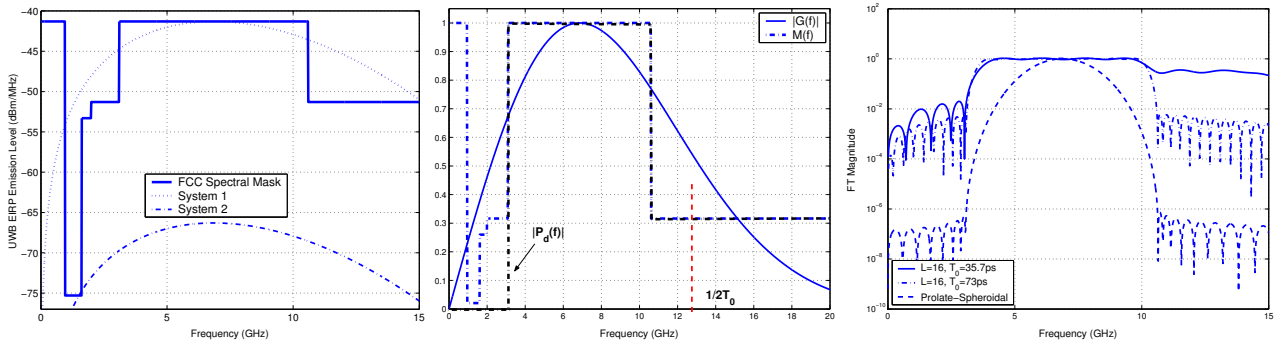


**Fig. 1.** *left:* FCC Spectral Mask; *center:*  $P_d(f)$  and  $\mathcal{M}(f)$ ; *right:* Fourier Transform of pulse shapers for single-band UWB.

$2L + 1$  coefficients, it then suffices to design  $L + 1$  taps  $\{w[n]\}_{n=0}^L$ , because upon defining  $w_0[n] = w[n + L]$ , we have  $W_0(e^{j2\pi F}) = \sum_{n=-L}^L w_0[n]e^{-j2\pi F n}$  being real, and  $|W_0(e^{j2\pi F})| = |W(e^{j2\pi F})|$ . The pulse design problem now is equivalent to:

Let  $\mathcal{F}$  represent the union of prescribed disjoint intervals in  $[0, 0.5]$ , so that  $D(F/T_0)$  is continuous in each interval. Choose taps  $\{w_0[n]\}_{n=0}^L$  that minimize  $\max_{F \in \mathcal{F}} |e(F)|$ , where  $e(F) := \lambda(F)[D(F/T_0) - W_0(e^{j2\pi F})]$  is the error function, and  $\lambda(F)$  denotes a positive weight function.

This problem is a classical Chebyshev approximation problem with desired function  $D(F/T_0)$ , and can be solved numerically based on the ‘‘Alternation Theorem’’ in polynomial approximation theory [9].

**Remark 1:** In addition to the widely-adopted Gaussian monocycle, any other readily available analog pulse shaper can be used as elementary building block in (4). This is because the functions  $D(f)$  we wish to approximate are normalized with respect to the FT of the elementary analog pulse shaper, namely  $G(f)$  for the Gaussian monocycle.

### 3.1. Single-Band UWB

In order to utilize the entire bandwidth,  $P_d(f)$  must be as in Fig. 1(*center*), where we have intentionally set  $P_d(f) = 0, \forall f < 3.1\text{GHz}$  to avoid interference to GPS. Recall also that the tap spacing  $T_0$  should be chosen with respect to the band region in which we want to control the pulse shaper. We will distinguish between the following two cases:

#### 3.1.1. Full Band Control

To gain full control over the entire band  $[3.1, 10.6]\text{GHz}$ , we select  $T_0$ , so that  $1/(2T_0) \geq 10.6\text{GHz}$ . The DTFT  $W(e^{j2\pi f T_0})$  then satisfies [c.f. (5)]

$$|W(e^{j2\pi f T_0})| : \begin{cases} \approx D(f) = \frac{P_d(f)}{|G(f)|} & f \in [0, \frac{1}{2T_0}] \\ < \frac{\mathcal{M}(f)}{|G(f)|} & \text{otherwise} \end{cases}. \quad (6)$$

Due to the periodicity of  $W_0(e^{j2\pi f T_0})$ ,  $T_0$  must be chosen so that  $|P(1/T_0 - 10.6)| < \mathcal{M}(1/T_0 - 10.6)$ , in order to satisfy condition (6). At the same time, we also want  $T_0$  to be as large as possible to ease implementation of (4).

Selecting  $T_0$  depends on  $\tau_g$  (or,  $f_g$ ). For instance, when  $f_g = 6.85\text{GHz}$ , we can choose  $1/(2T_0) = 14\text{GHz}$  and, ac-

cordingly,  $T_0 = 35.7\text{ps}$ . With  $T_0$  specified,  $D(F/T_0)$  is continuous within three intervals:  $\mathcal{I}_1 = (0, 3.1T_0)$ ,  $\mathcal{I}_2 = (3.1T_0, 10.6T_0)$ , and  $\mathcal{I}_3 = (10.6T_0, 0.5)$ . We choose  $\mathcal{F} = \bigcup_k \mathcal{F}_k$ , where  $\mathcal{F}_k \subset \mathcal{I}_k, \forall k = 1, 2, 3^1$ . With an appropriately selected weight function  $\lambda(F)$ , the optimum tap coefficients  $\{w[n]\}_{n=0}^{M-1}$  can be found and  $p(t)$  can thus be obtained via (4).

#### 3.1.2. Exploiting Symmetry to Halve the Clock Rate

We have seen that to design the optimal pulse shaper for a single-band UWB radio,  $T_0 = 35.7\text{ps}$  is required when  $f_g = 6.85\text{GHz}$ . Having full control over the entire bandwidth, we can design  $p(t)$  to closely approximate the FCC mask throughout the bandwidth. But this small  $T_0$  value may impose implementation difficulty. We will show next that sub-optimum alternatives are possible for single-band UWB with larger  $T_0$  (and thus smaller clock periods). With  $f_g = 6.85\text{GHz}$ , we can take advantage of the symmetry of  $D(f)$  in (6) and control  $P(f)$  only over the lower half of the entire band, by doubling the  $T_0$  value to  $T_0 = 73\text{ps}$ . This choice does not guarantee optimal approximation of the FCC mask over the entire bandwidth, unless  $D(f)$  is perfectly symmetric with respect to  $f = 6.85\text{GHz}$ . To approximate the normalized FT mask  $\mathcal{M}(f)$ , we set the desired function  $D_{sym}(f)$  to be:

$$D_{sym}(f) = \begin{cases} 0, & f \in [0, 3.1] \\ \min\{D(f), D(13.7 - f)\}, & f \in [3.1, 6.85] \end{cases},$$

where  $D(f)$  is the desired function in (6) and  $D_{sym}(F/T_0)$  is continuous in the intervals  $\mathcal{I}_1 = [0, 3.1T_0]$ , and  $\mathcal{I}_2 = [3.1T_0, 0.5]$ . We then choose the set  $\mathcal{F} = \bigcup_k \mathcal{F}_k$ , where  $\mathcal{F}_k \subset \mathcal{I}_k, \forall k = 1, 2$ . With the weight function  $\lambda(F)$  being chosen appropriately, the pulse shaper can be readily designed.

### 3.2. Multi-Band UWB

As we mentioned before, partitioning the ultra-wide bandwidth into sub-bands facilitates FH, which is important for enhancing user capacity and robustifying LPI/LPD. On the other hand, it is desirable to avoid adjacent channel interference in multi-band UWB systems by confining the spectrum

<sup>1</sup>The transition interval should be appropriately selected, otherwise, the designed filter length will be large when small approximation error is desired

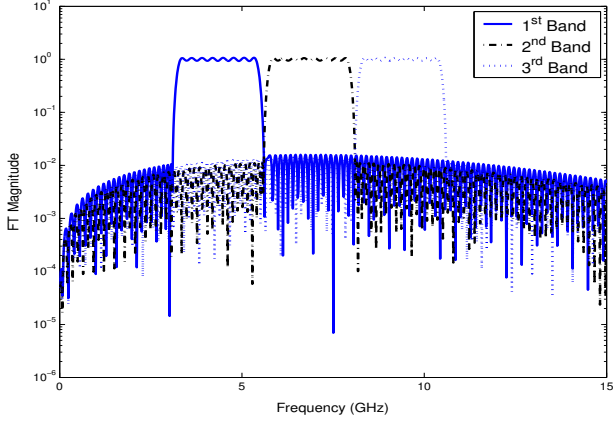


**Fig. 2.** Fourier Transform of pulse shapers for multi-band UWB.

of each channel within its prescribed band, while still efficiently utilizing the FCC spectral mask.

Similar to the single-band pulse design, the tap spacing  $T_0$ , can be selected, depending on whether full-band (3.1 – 10.6GHz) or half-band (3.1 – 6.85GHz) control is required. With full-band control, the desired functions  $\{D_i(f)\}_{i=0}^{N-1}$ , each corresponding to one of the total  $N$  sub-bands, are

$$D_i(f) = \begin{cases} \frac{P_a(f)}{|G(f)|} & f \in 3.1 + i\frac{7.5}{N} + [0, \frac{7.5}{N}] \text{GHz} \\ 0 & \text{otherwise} \end{cases} \quad (7)$$

Based on (7), pulse shapers can be designed for multi-band UWB by appropriately choosing  $\lambda(F)$  and  $\mathcal{F}$ .

It is worth mentioning that with the same number of sub-bands  $N$ , full-band control results in  $N$  FH slots, whereas half-band control only results in  $N/2$  FH slots. Clearly, on top of this optimality-complexity tradeoff, there is also a user capacity-complexity tradeoff.

**Remark 2:** As we mentioned before, it is sometimes desirable to use only a fraction of the entire bandwidth in order to avoid NBI, or, the highly-lossy high-frequency bands. In such cases, parameters  $T_0$ , and  $\{w[n]\}_{n=0}^{M-1}$  can be flexibly selected to meet desirable spectral specifications.

#### 4. NARROW-BAND INTERFERENCE ISSUES

To minimize interference to and from co-existing services, our pulse shapers can be designed to impose minimum energy leakage to a prescribed band. Next, we quantify the impact our pulse shaper designs have on the bit error rate (BER).

**Proposition 1** *In a single-user UWB link over an AWGN channel that includes NBI, with binary PPM and TH as in (1), the average BER with a correlation receiver is:*

$$P_e = Q\left(\sqrt{\frac{N_f \mathcal{E}}{N_0(1 + \alpha \frac{J_0}{N_0})}}\right) \quad (8)$$

where  $N_0/2$  is the AWGN variance,  $J_0/2$  is the PSD of the NBI over the frequency band  $[f_L, f_U]$ , and  $\alpha := \int_{f_L}^{f_U} |H(f)|^2 df / N_f$ , with  $H(f)$  being the FT of  $h(t) := \sum_{n=0}^{N_f-1} [p(t - nT_f) - p(t - nT_f - \Delta)]$ .

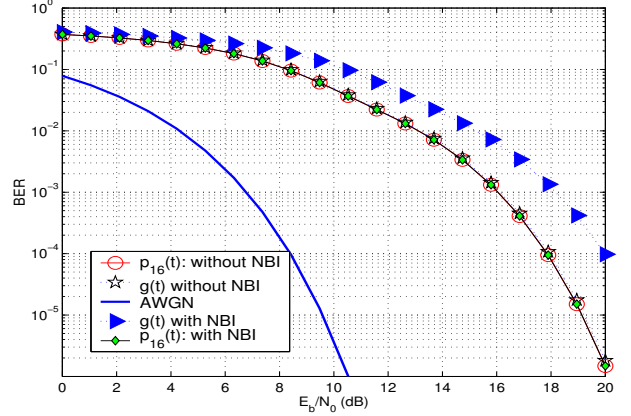


**Fig. 3.** Comparisons with NBI.

Eq. (8) shows that  $\alpha$  affects BER performance by altering the effective SNR. And  $\alpha$  is merely determined by the pulse shaper  $p(t)$ . With our pulse design algorithm, we can easily shape our pulse with minimum energy leakage into the NBI band  $[f_L, f_U]$ , and thus reduce BER.

In the presence of multipath effects, NBI can be mitigated similarly by designing pulse shapers with smaller  $\alpha$  values. This is possible because even in the presence of multipath, the variance of the received NBI term is reduced in exactly the same way as for AWGN channels. We will also verify this by simulations when comparing the BER performance in the presence of multipath in Section 6.4.

### 5. IMPLEMENTATION ISSUES

To implement our pulse shaper designs in (4), currently available hardware is sufficient: a Gaussian monocycle generator, and a shift register that stores the tap coefficients.

#### 5.1. Digital Sub-band Hopping

As we discussed earlier, our pulse shaper design can also support multi-band UWB transmissions with FH. To hop from one sub-band to another, one can simply reset the memory of the shift register, or, use a bank of shift registers and switch among them to select the desired band. Notice that this digital architecture implements linear combinations of the base-band Gaussian monocycle, and does not involve analog carriers. This avoids CFO effects commonly encountered with analog FH. The limitation of the proposed architecture is the relatively stringent requirement on the clock timing accuracy, which is up to several picoseconds. Also, clock jitter phenomena could impair BER performance in our design.

#### 5.2. Clock Jitter Effects

To implement our designs, the clock must maintain picosecond accuracy, which can be provided by existing PulsON technology from Time Domain Corporation [10]. Thanks to the digital implementation of our design method, even when the timer is imperfect, the tap coefficients can be easily adjusted to satisfy the FCC spectral mask.

With regards to the average error performance in the pres-

ence of clock jitter, we have established the following [7]:

**Proposition 2** *In a single-user UWB link over AWGN channels, and clock jitter uniformly distributed over  $[-\beta, \beta]$  with  $\beta \ll T_g$ , the average received SNR can be approximated by:  $\gamma = \frac{\mathcal{E}}{N_0} [1 - \mathcal{C}\beta^2 + O(\beta^3)]$ , where  $\mathcal{C} \geq 0$  is a constant.*

So long as the clock jitter  $\beta$  remains small, it will not cause a major SNR reduction. With independent jitters  $\{\epsilon_k\}_{k=0}^{M-1}$  in (4), the pulse shaper becomes  $\tilde{p}(t) = \sum_{k=0}^{M-1} w[k]g(t - kT_0 - \epsilon_k)$ . For its random FT  $\tilde{P}(f)$ , we have shown that  $E\{|\tilde{P}(f)|^2\} = (1 - (\frac{\sin(2\pi f\beta)}{2\pi f\beta})^2) \sum_{k=0}^{M-1} w^2[k] + |P(f)|^2 (\frac{\sin(2\pi f\beta)}{2\pi f\beta})^2$ , which is well approximated by  $|P(f)|^2$  when  $\beta \ll T_g$ .

As clock jitter is present in our baseband designs, frequency jitter is present in carrier-modulated systems too. The average received SNR is related to the CFJ  $f_J$ , when assumed to be uniformly distributed over  $[-\xi_0, \xi_0]$ , is:  $\gamma = \gamma_0 \left( \frac{1}{2} + \frac{\sin(4\pi\xi_0 t)}{8\pi\xi_0 t} \right)$ , with  $\gamma_0$  denoting the SNR in the absence of CFJ/CFO. From this expression, we deduce that even a small  $f_J$  will cause considerable degradation in the average SNR as  $t$  increases.

## 6. DESIGN EXAMPLES AND COMPARISONS

In this section, we apply the approach of Section 3 to design pulse shapers for single- and multi-band UWB systems. The Gaussian monocycle parameter  $f_g$  is chosen to be 6.85GHz.

**6.1. Single-Band UWB** ( $T_0 = 35.7\text{ps}$  and  $73\text{ps}$ ): We choose the sets  $\{\mathcal{F}_k\}_{k=1}^3$  in Section 3.1.1 to be  $[0, 0.1107]$ ,  $[0.15, 0.33]$ , and  $[0.3786, 0.5]$ , respectively. The weight  $\lambda(F)$  is 2 for  $F \in \mathcal{F}_1$ , and 1 otherwise. We weigh more the band  $\mathcal{F}_1$  to minimize the energy inside  $\mathcal{F}_1$ . With  $L = 16$  ( $M = 33$ ), the designed  $p(t)$  and its FT are shown in Fig. 1(right).

Next, we select the sets  $\mathcal{F}_1, \mathcal{F}_2$  in Section 3.1.2 to be  $[0, 0.2263]$  and  $[0.28, 0.5]$ , respectively. The weight  $\lambda(F)$  is now 5 in  $\mathcal{F}_1$ , and 1 otherwise. With  $L = 16$ , the resulting pulse has duration  $T_p = 2.52\text{ns}$ , and is depicted along with its FT in Fig. 1(right).

**6.2. Multi-Band UWB** ( $T_0 = 35.7\text{ns}$ ): Here, we design pulse shapers for  $N = 3$  sub-bands. The desired functions,  $D_i(f), i = 0, 1, 2$ , are as in (7). In the design process, we choose the set  $\mathcal{F}$  to be  $[0, 0.1107] \cup [0.1178, 0.1928] \cup [0.2, 0.5]$  for the 1<sup>st</sup> band,  $[0, 0.2] \cup [0.0.2071, 0.2821] \cup [0.2892, 0.5]$  for the 2<sup>nd</sup> band, and  $[0, 0.2892] \cup [0.2964, 0.3714] \cup [0.3785, 0.5]$  for the 3<sup>rd</sup> one. The weight  $\lambda(F)$  is 5 over  $\mathcal{F}_2$ , and 1 otherwise. With  $L = 100$ , the optimal pulse shapers and their FTs are shown in Fig. 2.

**6.3. Power Efficiency Comparison:** As we discussed in Section 2, for any pulse shaper  $p(t)$ , compliance to the FCC mask can be achieved by adjusting the transmit energy per pulse  $\mathcal{E}$ , or equivalently, the transmit power. We will compare the maximum allowable transmit power limited by the FCC mask corresponding to three pulse shapers: (i) the Gaussian monocycle  $g(t)$  with  $f_g = 6.85\text{GHz}$ ; (ii) the pulse shaper

$p_{16}(t)$  we designed in Section 3.1.1 with  $T_p = 1.3\text{ns}$ ; and (iii) the ‘‘prolate-spheroidal’’ pulse shaper  $p_{p-s}(t)$  designed in [3] with  $T_p = 1.3\text{ns}$ .

With  $G(f), P_{p-s}(f)$ , and  $P_{16}(f)$  denoting the corresponding FTs, the EIRP spectra of these three pulses are  $|G(f)|^2/T_f$ ,  $|P_{p-s}(f)|^2/T_f$ , and  $|P_{16}(f)|^2/T_f$ . Complying with the FCC spectral mask, while transmitting at the maximum allowable power, these pulses need to be scaled so that (see also Fig. 1(center)):

$$\begin{aligned} |\theta_1 G(f)|^2/T_f &\leq -66.3\text{dBm/MHz}, \\ |\theta_2 P_{p-s}(f)|^2/T_f &\leq -41.3\text{dBm/MHz}, \\ |\theta_3 P_{16}(f)|^2/T_f &\leq -41.3\text{dBm/MHz}, \end{aligned}$$

where  $\theta_1, \theta_2, \theta_3$  are scaling factors. Accordingly, their corresponding maximum transmit powers are:  $\mathcal{P}_g = 0.00387\text{mW}$ ,  $\mathcal{P}_{16} = 0.91\text{mW}$ , and  $\mathcal{P}_{p-s} = 0.25\text{mW}$ , respectively. It is clear that our design utilizes the FCC spectral mask most efficiently.

**6.4. Comparisons with NBI:** In the presence of a multipath channel, with  $J_0 = 10N_0$  in the band  $0.96-3.1\text{GHz}$ , we compare the UWB system performance with two different pulse shapers:  $p_{16}(t)$  and  $g(t)$  with  $f_g = 6.85\text{GHz}$ . The multipath channel is generated according to the Saleh-Valenzuela model, with parameters  $(\Lambda, \lambda) = (0.0233, 2.5)\text{ns}^{-1}$ , and  $(\Gamma, \gamma) = (7.1, 4.3)\text{ns}$ . We choose  $N_f = 32$ ,  $\Delta = 1.5\text{ns}$ ,  $T_c = 4\text{ns}$ , and  $T_f = 100\text{ns}$ . A 16-finger RAKE with spacing  $\geq 2\text{ns}$  is used with MRC. In the absence (presence) of NBI, the BER performance of the UWB system with different pulse shapers is plotted in Fig. 3. Clearly, our designed pulse shaper mitigates NBI better than the Gaussian monocycle.

## 7. REFERENCES

- [1] R. A. Scholtz, ‘‘Mutiple Access with Time Hopping Impulse Modulation,’’ *MILCOM*, Boston, 1993, pp. 447-450.
- [2] P. Withington, ‘‘Impulse Radio Overview,’’ Time Domain Corp., <http://user.it.uu.se/~carle/Notes/UWB.pdf>
- [3] B. Parr, B. Cho, K. Wallace, Z. Ding, ‘‘A Novel Ultra-Wideband Pulse Design Algorithm,’’ *IEEE Comm. Letters*, pp. 219-221, 2003.
- [4] J. Romme, L. Piazza, ‘‘On the Power Spectral Density of Time-Hopping Impulse Radio,’’ *UWBST*, Baltimore, pp. 241-244.
- [5] J. D. Taylor, *Ultra Wideband Radar Technology*, CRC Press, New York, 2002.
- [6] F. Ramirez-Mireles, R. A. Scholtz, ‘‘System Performance Analysis of Impulse Radio Modulation,’’ *Radio and Wireless Conf.*, Colorado Springs, 1998, pp. 67-70.
- [7] X. Luo, L. Yang, and G. B. Giannakis, ‘‘Designing Optimal Pulse-Shapers for Ultra-Wideband Radios,’’ *J. of Comm. and Networks*, submitted, July 2003.
- [8] J.S. Lee, C. Nguyen, T. Scullion, ‘‘New Uniplanar Subnanosecond Monocycle Pulse Generator and Transformer for Time-Domain Microwave Applications,’’ *IEEE Trans. on MTT*, pp. 1126-1139, 2001
- [9] T. W. Parks, J. H. McClellan, ‘‘Chebyshev Approximation for Nonrecursive Digital Filters with Linear Phase,’’ *IEEE Trans. on Circuit Theory*, pp.189-194, 1972.
- [10] D. Kelly, S. Reinhardt, R. Stanley, M. Einhorn, ‘‘PulsON Second Generation Timing Chip: Enabling UWB Through Precise Timing,’’ *UWBST*, Baltimore, 2002, pp. 117-121.